Amping Up, Saving Power

<AU: Please note that the following is for the ToC only and will not appear in the article itself. It will, however, be searchable in Xplore.>

Digital Predistortion Linearization Strategies for Power Amplifiers Under Wideband 4G/5G Burst-Like Waveform Operation

David López-Bueno, Teng Wang, Pere L. Gilabert, and Gabriel Montoro

Fourth-generation (4G) communication systems based on orthogonal frequency division multiplexing (OFDM) and the proposed backwards compatible fifth-generation (5G) variants, like filter-bank multi-carrier (FBMC), are based on modulation techniques that allow significantly increased spectral efficiency and capacity in mobile radio access networks (RANs). However, the use of these modulation techniques impacts the requirements of the radio base stations, which have been traditionally the most energy consuming-element of mobile networks, accounting for up to 80% of the energy consumption of RANs [1]. Non-constant envelope-modulation techniques with high peak-to-average power ratios (PAPRs) require highly linear power amplifier (PA) amplitude and phase responses to fulfill stringent spectral mask and modulation accuracy requirements. This is often achieved with significant PA back-off, which considerably reduces PA efficiency because the PA's maximum efficiency is achieved near the saturation point.

The adoption of gallium nitride (GaN) PA technologies and use of digital linearization techniques are playing a key role in building more efficient base-

David López-Bueno (david.lopez@cttc.es) is with Phycom Dept., Centre Tecnològic de Telecomunicacions de Catalunya (CTTC) and Universitat Politècnica de Catalunya (UPC) pursuing a Phd, Parc Mediterrani de la Tecnologia, Castelldefels, Spain. Teng Wang (teng.wang@estudiant.upc.edu), Pere L. Gilabert (plgilabert@tsc.upc.edu), and Gabriel Montoro (gabriel.montoro@upc.edu) are with the Dept. of Signal Theory and Communications, Universitat Politècnica de Catalunya (UPC), c/ Esteve Terradas, 7, 08860, Castelldefels, Spain.

Digital Object Identifier 10.1109/MMM.2015.2488338
Date of publication:

station and backhaul radios. GaN devices feature improved linearity and power-conversion efficiency, and higher RF power densities, switching speeds, and bandwidth (BW) at a smaller size and required heat sink. By combining GaN PA devices with digital processing techniques such as crest-factor reduction (CFR) and digital predistortion (DPD), the classical linearity versus power efficiency tradeoff can be mitigated for wireless infrastructure equipment dealing with high PAPR waveforms.

CFR reduces the peaks of the modulated waveform to a satisfactory level to better enable the use of the PA. Due to in-band and out-of-band distortion, CFR does not introduce system gain; but, thanks to reduction in the peaks, it is possible to operate the PA at higher average power and therefore closer to its saturation point, where it is most efficient. CFR is combined with DPD in order to mitigate the PA distortion and maximize the power efficiency.

DPD relies on digitally cascading a nonlinear system before the PA, which provides an inverse response to the PA that then provokes a linear response at the output of the cascaded system, including the PA [2]. These techniques may have a positive impact at product level due to the following:

- First, because the transmit (Tx) system linearity is improved, these techniques allow the use of cost-effective and lower-power-consuming PA solutions with less expensive board, enclosure, and heat sink designs as well as simplified power supply and cooling subsystems.
- Second, by combining DPD and CFR, system performance can be enhanced therefore extending the reach and robustness against interference of radio access equipment, which maximizes the system efficiency [2].
- Third, closed-loop DPD may enable transmitter self-calibration and correction performance, thereby reducing the product validation and yield costs, increasing its operating stability, and minimizing the number of maintenance operations.

DPD Competition Details

At the 2015 IEEE Microwave Theory and Techniques Society (MTT-S) International Microwave Symposium, the student design competition in the category PA Linearization through Digital Predistortion, jointly sponsored by MTT-9 Technical Committee on Digital Signal Processing and MTT-11 Technical Committee on Microwave Measurments [3], was an excellent opportunity for the competing teams to deploy DPD strategies to linearize a GaN PA in a scenario that could fit 4G or future 5G radio base stations operating with high-PAPR OFDM-based burst-like waveforms.

The student teams had to predistort 40-MHz BW signals at the output of a GaN PA operating at a 2.14-GHz carrier frequency and showing substantial memory effects due to trapping phenomena [4]. To evaluate the effectiveness of the predistortion schemes, the organizers provided the following formula:

$$\text{SCORE} = -\left(\begin{matrix}\text{NMSE}_{\text{weighted}} + 5 \times \max(\text{ACPR} + \\ 50,0) + 5 \times \text{abs}(\text{Pout}_{\text{dBm}} - 27)\end{matrix}\right). \quad (1)$$

The first figure of merit is the $\text{NMSE}_{\text{weighted}}$, which is a normalized mean square error calculation quantifying the likelihood estimate between the baseband Tx waveform before applying any digital linearization technique and the baseband received (i.e., post-PA down-converted and time aligned) waveform. The second figure of merit is the adjacent channel power ratio (ACPR) that quantifies the worst-case power

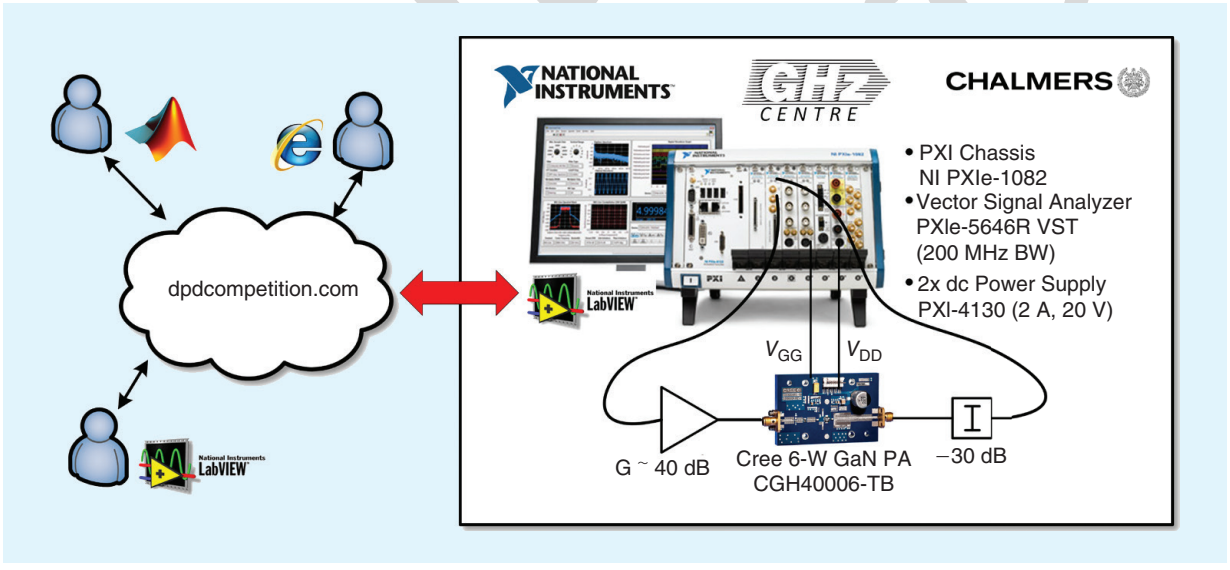

Figure 1. *The DPD competition measurement setup from [4].*

ratio between any of the adjacent channels and the main channel and therefore accounts for the spectral regrowth due to the PA distortion. The third figure of merit is the mean power level reached at the output of the PA. The score is penalized if the target values of −50-dBc ACPR and +27-dBm output power level are not met.

The measurement setup in Figure 1 consists of a National Instruments modular PXI platform with an embedded host PC controller, a 65-MHz–6 GHz vector signal transceiver (VST) featuring 200-MHz maximum instantaneous BW, and two dc power supplies. The maximum signal BW was limited to 160 MHz to avoid distortion in the signal generation process and filtering at reception. Between the RF Tx and Rx ports of the VST, a 40-dB linear driver amplifier is followed by the Cree 6W GaN PA testboard that has to be linearized; a 30-dB attenuator is placed at the output to lower the PA level to the VST.

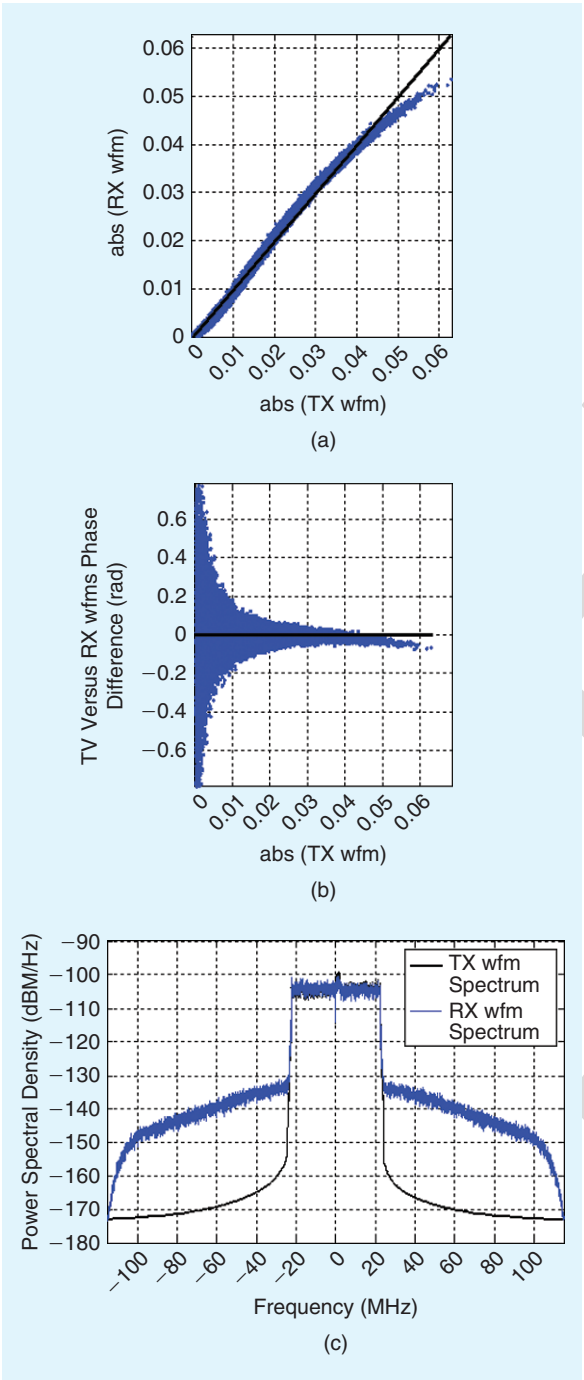

Figure 2. *Evaluations of the GaN PA's linear performance [Tx versus Rx waveforms (WFMs)] with statistically representative test signalS: (a) AM-AM, (b) AM-PM, and (c) conversion and power spectral density.*

The embedded PC is in charge of interfacing with the PXI VST and dc power modules. A key feature of the measurement setup is the ability to enable remote operation through an Internet connection. The overall platform is called the WebLab [4] and was made available by the GigaHertz Center at the Microwave Electronics Lab at Chalmers University of Technology, Gothenburg, Sweden. Some MATLAB scripts are available to facilitate the generation, upload, and download of waveforms and calculate the score.

Initial Measurement Setup Considerations

We built a statistical characterization block giving information about the waveform PAPR distribution that stores test signals for predefined PAPR ranges of interest. Test signals having a PAPR of around 13.5 dB (the PAPR distribution is shown later in the article) will be used to have statistical significance. Once desirable test signals are made available, the initial characterization of the PA through the measurement setup is performed by observing the AM (amplitude modulation)-AM and AM-PM (phase modulation) characteristics, the spectral shape (see Figure 2), and measurement parameters such as the normalized mean square error (NMSE) and the adjacent channel power atio (ACPR). To evaluate this data, proper time alignment between the Tx and receive (Rx) waveforms is required. To find the fractional time delay between them, the two waveforms were upsampled by 100, time-aligned by means of a circular cross-correlation, and downsampled by 100.

Preliminary Digital Linearization Architecture

In a DPD scheme, three relevant aspects need to be taken into account: the PA behavioral model being used, the parameter estimation architecture, and the parameter estimation method. We have evaluated the memory polynomial (MP) [5], dynamic-deviation-reduction-based Volterra (DDR-Volterra) [6], and generalized memory polynomial (GMP) [7] models. GMP has been chosen since it outperformed MP and DDR-Volterra in our scenario. For parameter estimation, our DPD scheme followed the direct learning (DL) approach [8], using the linear least squares (LS) solution as the estimation method because while the DPD function is nonlinear, it is linear in the parameters. DL was chosen instead of the simpler and widely used

indirect learning architecture because it performs better [9]–[10].

The initial MATLAB testbench and DPD architecture and formulation to combat the GaN PA nonlinearities are shown in Figure 3, where it can be seen that the DL parameter extraction follows a closed-loop architecture employing the feedback signal $y[n]/G_0$

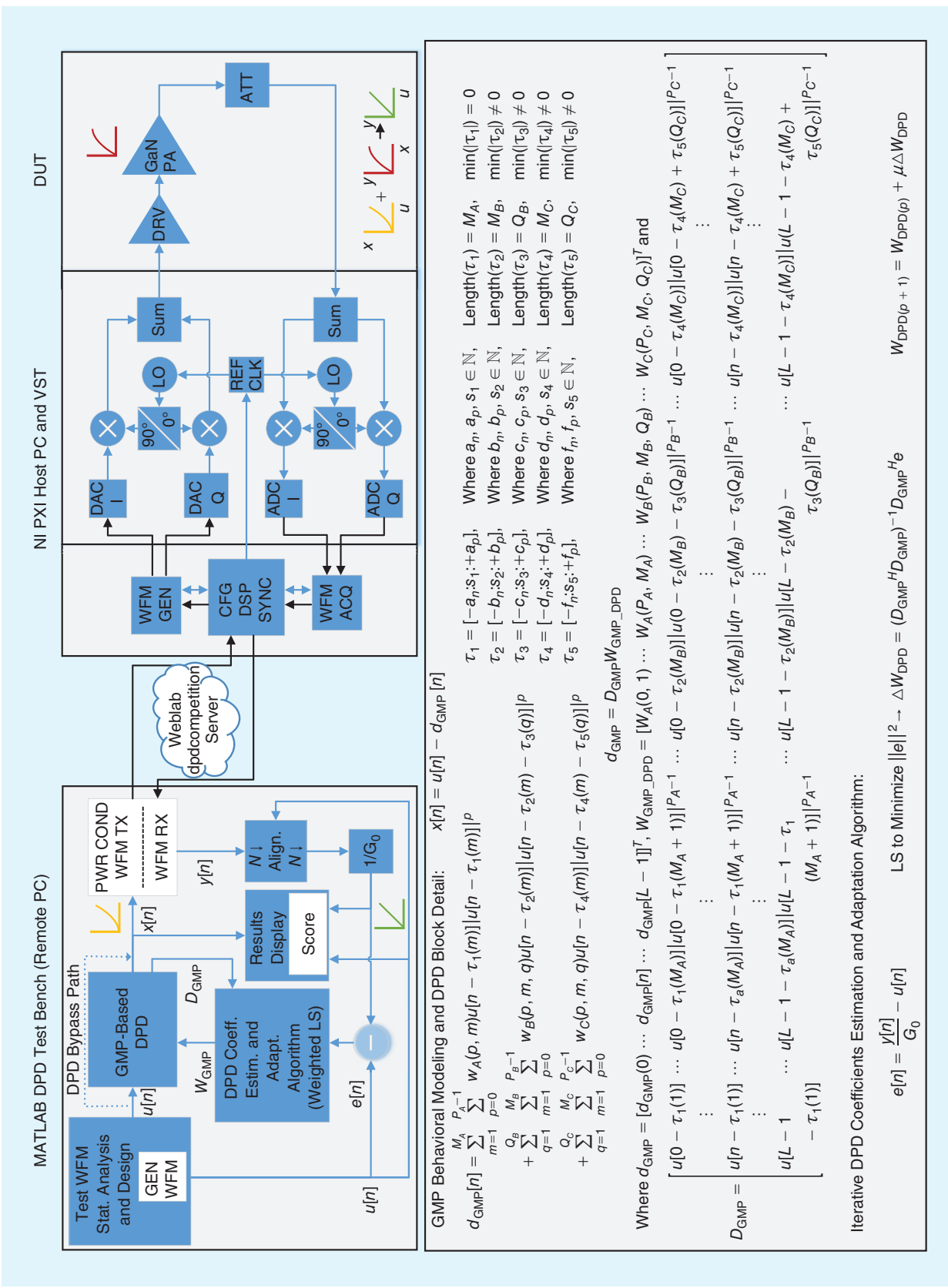

Figure 3. *The DPD closed-loop adaptive architecture and formulation based in DL parameter estimation. CFG: control-flow graph; DSP: digital signal processor; ADC: analog-to digital convertor; LO: local oscillator; REF CLK: reference clock; DRV: drive; ATT: attentuator.*

(G_0 being the linear gain of the PA) together with the input signal u[n] to extract the DPD coefficients.

The predistorted signal $x[n]$ is derived from subtracting the distortion signal $d_{GMP}[n]$ to the original signal $u[n]$, both having L samples, in the GMP behavioral modeling and DPD block. The classical GMP formulation to provide $d_{GMP}[n]$ is shown in Figure 3. The first term is the MP expression having $P_A M_A$ DPD coefficients; the second and third terms introduce both negative and positive cross-term delays to the MP model, having $P_B M_B Q_B$ and $P_C M_C Q_C$ coefficients, respectively ($P_{A|B|C}$ are polynomial orders, while $M_{A|B|C}$ and $Q_{B|C}$ relate to memory depths). The GMP expression is reformulated using vector notation in Figure 3.

In order to calculate the DPD coefficients, the $\boldsymbol{D}_{GMP}$ matrix is sent to the DPD coefficient estimation and adaptation block. This block iteratively calculates the DPD coefficients $\boldsymbol{w}_{GMP}$ toward minimizing the difference between the original signal $u[n]$ and the received signal (taken at the PA output), after proper alignment and accounting for the linear gain G_0, by using LS. With the closed –loop DL architecture employed, the coefficients from a previous estimate are used and partially updated with a weighting factor μ (between 0 and 1) that decreases with the number of iterations. The DPD coefficients are finally sent to the DPD block, which calculates d[n] and the resulting predistorted signal.

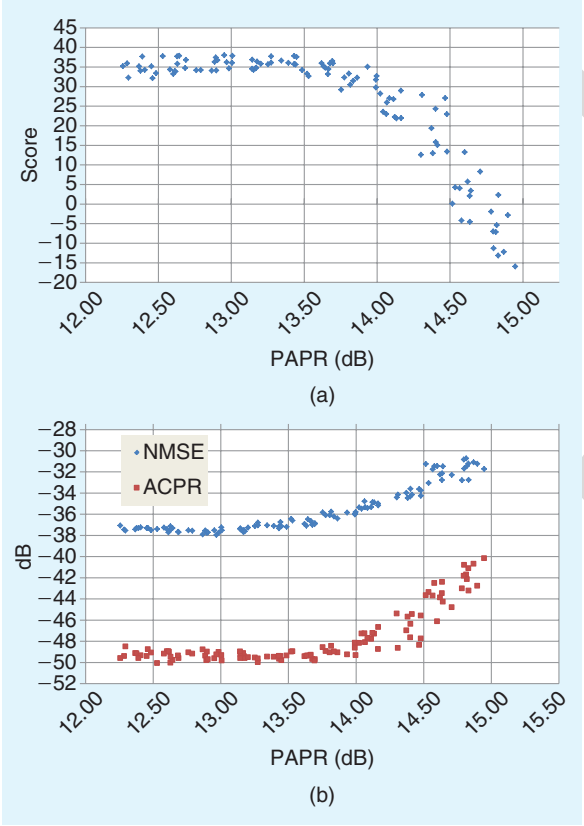

Figure 4. *(a) The score scatter plot and (b) the NMSE and ACPR for 100 Weblab experiments.*

With the previous architecture, multiple experiments with the Weblab have been conducted in order to tune the best GMP parameters and have the best coefficients after training the DPD for the statistically representative signals. The coefficients are stored and used against different PAPR test signals to evaluate the stability of the score for similar PAPR range signals and the degradation suffered when signals with higher PAPR are employed, to estimate the impact of potential cases used in the final competition. Figure 4 displays the score, NMSE, and ACPR values after conducting a measurement campaign.

The results show that for test waveforms with PAPR of up to 13.5 dB, the NMSE and ACPR values are reasonably stable, but small variations in the ACPR lead to visible variations in the score (i.e., up to between five and six points). Considering that the mean output power levels are stable and very close to the +27 dBm goal, some further work is required to improve the NMSE by a few dB and push the ACPR to values below −50 dBc to increase the score and reduce its variance. For waveforms with PAPR 13.5–14 dB, a slight degradation and increase in the variance of the performance is noticed. Beyond 14-dB PAPR values, degradation in the score is produced because the NMSE and, more importantly, the ACPR decrease significantly, which demands mitigation countermeasures.

Techniques Targeting Performance and Results Stability

Decomposed, Piecewise GMP/MP DPD Modeling

The AM-AM characteristic of the PA in Figure 2 shows a different behavior according to the amplitude (or alternatively, power) level. At low amplitude levels, we observe some gain expansion, while at high amplitude levels, gain compression occurs. Since high amplitude values occur less frequently, a simplified (in terms of memory taps) behavioral model can be considered, which favors the robustness of the extracted DPD coefficients.

First, the input signal was decomposed into two subsignals, as shown in Figure 5(a). Following the same principle presented in [11], we introduced piecewise curve-fitting, dividing the DPD function into two segments for high and low input amplitude levels. The segment of low amplitude values was modeled with the previously detailed GMP model, while for the high amplitude values we relaxed the complexity by using a MP model as seen in (2).

$$\boldsymbol{d}_{PW} = \boldsymbol{D}_{GMP}^{low} \boldsymbol{w}_{GMP} + \boldsymbol{D}_{MP}^{high} \boldsymbol{w}_{MP}. \quad (2)$$

Long-Term Memory Effects Modeling

By taking into account the bursty nature of the test signal, we considered the possibility of also modeling

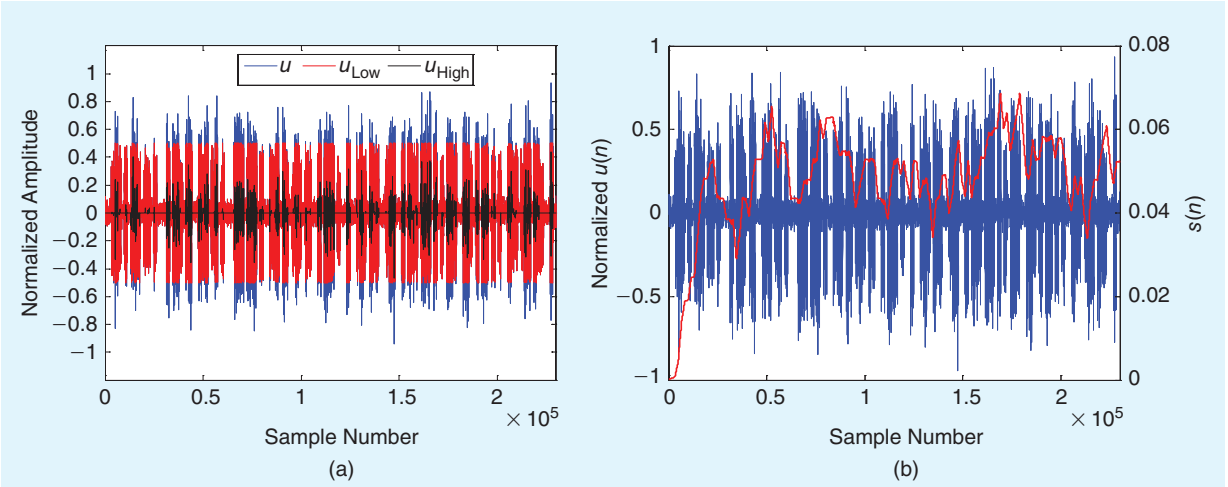

Figure 5. *(a) Waveform decomposition into high and low values for a 0.5 amplitude threshold and (b) extraction of the long-term variable following the waveform power dynamics.*

long-term memory effects. The memory effects make the output of a power amplifier at a given time depend not only on the on the present input value but also on previous output and input values. The bursty nature of the PA input signal may induce dynamic effects such as bias circuit modulation, self-heating, and charge-trapping phenomena that feature time constants much larger than the period of the RF carrier frequency (and fall closer to the time scale of the envelope or modulation signal [12]), which are not tracked by the DPD coefficients unless a long-term dependence is introduced in the estimation process.

Following the same principle presented in [13], an estimate of the long-term variable was created (s[n]), consisting of the average input power over a finite window. The number of samples chosen to define the window determines the long-term memory depth.

$$s[n] = \frac{1}{N}\sum_{i=0}^{N-1} |u[n-i]|^2. \tag{3}$$

Considering the previous decomposed, piecewise modeling and the long-term memory effects, the nonlinearities are modeled as follows:

$$\begin{aligned} \boldsymbol{d}_{\mathrm{PW,LT}} &= \boldsymbol{D}^{\mathrm{low}}_{\mathrm{GMP}}\boldsymbol{w}_{\mathrm{GMP}} + \boldsymbol{D}^{\mathrm{high}}_{\mathrm{MP}}\boldsymbol{w}_{\mathrm{MP}} + s[n] \\ \boldsymbol{D}_{\mathrm{GMP}}\boldsymbol{w}_{\mathrm{GMP,LT}} &= \boldsymbol{D}^{\mathrm{low}}_{\mathrm{GMP}}\boldsymbol{w}_{\mathrm{GMP}} + \boldsymbol{D}^{\mathrm{high}}_{\mathrm{MP}}\boldsymbol{w}_{\mathrm{MP}} + \\ &\quad \boldsymbol{D}^{\mathrm{long}}_{\mathrm{GMP}}\boldsymbol{w}_{\mathrm{GMP,LT}} \end{aligned}. \tag{4}$$

The number of coefficients grows significantly when taking into account all the features described (e.g., hundreds of coefficients). Model order reduction techniques such as the ones based on the principal component analysis (PCA) theory may be very useful in simplifying the computational complexity of the DPD [14].

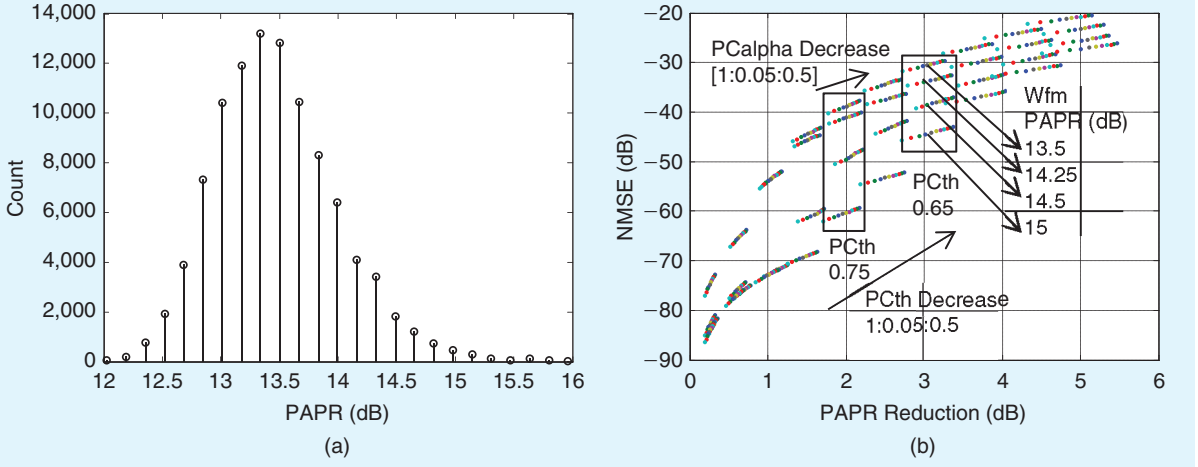

Figure 6. *(a) The OFDM-like waveform PAPR distribution (25 bins, 100,000 iterations) and (b) the NMSE versus CFR reduction for different PC thresholds and alpha for 13.5 dB, 14.25 dB, 14.5 dB, and 15 dB PAPR test signals.*

Waveform Expansion and Mesh-Selecting

The optimality of the extracted DPD coefficients using LS strongly depends on the number of samples used in the computation. A priori, the LS estimator may need a large number of data samples (or equations) to obtain the best approximation of the coefficients. From a computational complexity point of view, we want the number of data samples be as small as possible. However, using short sequences of data samples leads to [15]

1) the ill-conditioning problem due to the rank deficiency of LS matrices
2) the statistical mismatch problem, because the short data sequence often cannot fully represent the statistical property of the input domain (accuracy problem).

Assuming that our data matrix has no problems of rank deficiency, we can address the accuracy problem by extending the number of observations (i.e., extending the number of required waveforms to N, shown later in Figure 7) before extracting the DPD coefficients with the LS algorithm, and then by selecting those samples that are more statistically representative of the input domain for each of the observation waveforms. With the so-called mesh-selecting method [16], given a fixed length of data (rows of the data matrix), we can extend the number of observations and, after proper selection of the most statistically representative data, build the data matrix providing robustness to the DPD parameter extraction.

Peak Cancellation Crest-Factor Reduction

CFR has been used as protection to minimize the effects of having a signal with PAPR larger than the statistical mean value at which the predistorter has been previously trained during final tests (to avoid highly penalizing ACPR degradation). The peak cancellation (PC) technique described in [17] has been chosen as a clipping and filtering CFR method.

The PC algorithm employs different A (threshold) and α (subtraction factor) settings according to preestablished PAPR ranges to optimize the ACPR values without significant NMSE degradation for each of the cases. Figure 6(a) shows the PAPR distribution for 100,000 waveforms created with the MATLAB func-

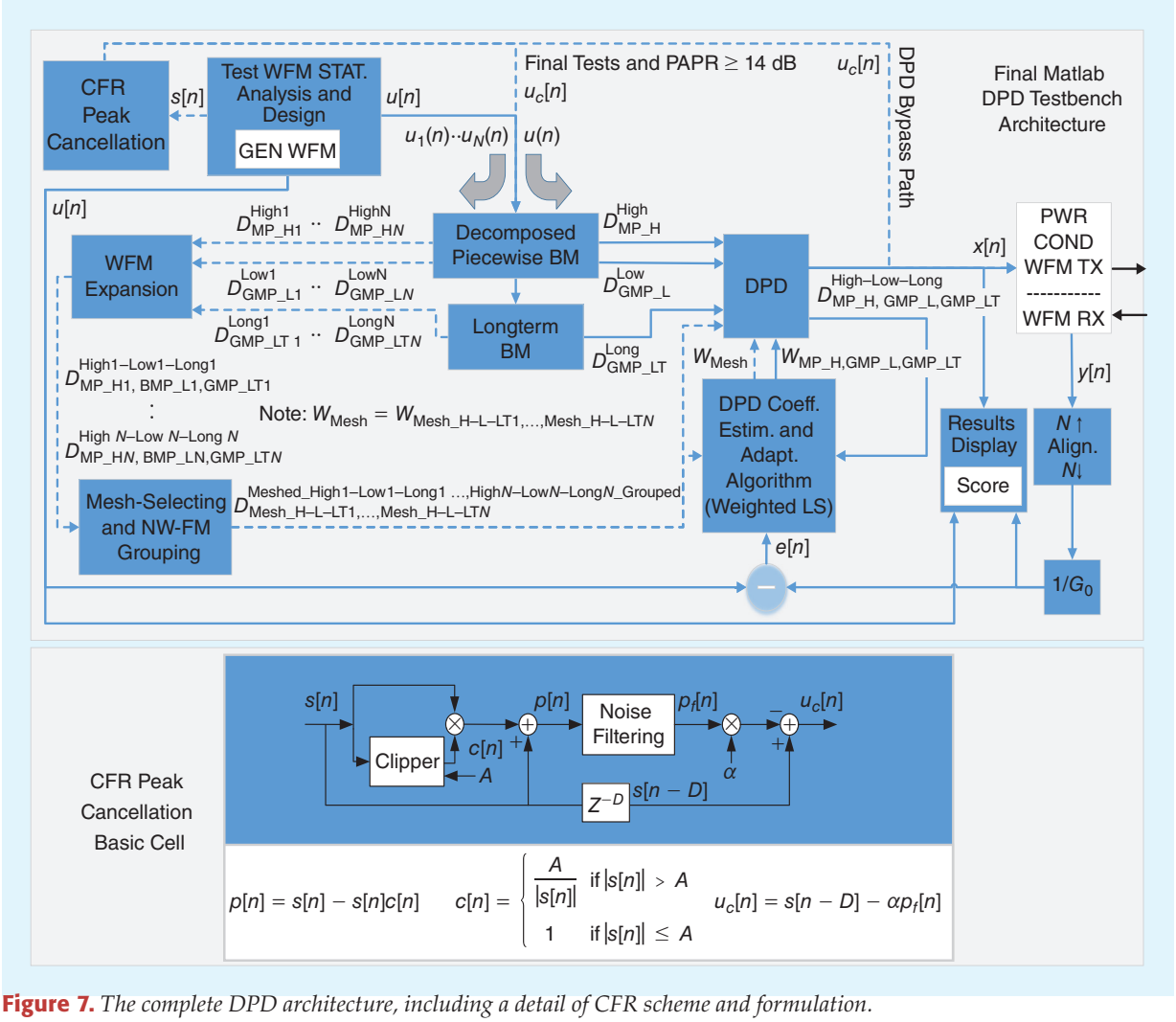

Figure 7. *The complete DPD architecture, including a detail of CFR scheme and formulation.*

tion made available to generate the DPD competition OFDM-like signals. The plot in Figure 6(b) shows the NMSE degradation versus PAPR reduction for different PAPR signals (parallel grouped lines) and the threshold and subtraction factor values (from 1 to 0.5 in 0.05 steps), helping to set desirable PC configurations for each PAPR range according to a specific maximum allowed NMSE degradation.

The five stages of the basic PC cell shown in Figure 7 (bottom) have been used before entering the DPD blocks and applying the coefficients.

Overall Digital Linearization Architecture and Final Competition Approach

The final DPD architecture to face the challenges of the competition is shown in Figure 7. After analyzing the measurement process, one can see that the results show now much better stability. The score mean has been improved three to four points, as seen in Figure 8(a) **<Au: Please make sure that Figure 8 text references are accurate as edited.>** and is above 40 points for PAPRs below 14 dB.

The final competition provided each competitor 15 minutes to, first, adjust the initial power level after measuring the gain and then tune the predistorter gain (i.e., in the DL and weighted LS methods) with a short training, and, second, perform the best DPD

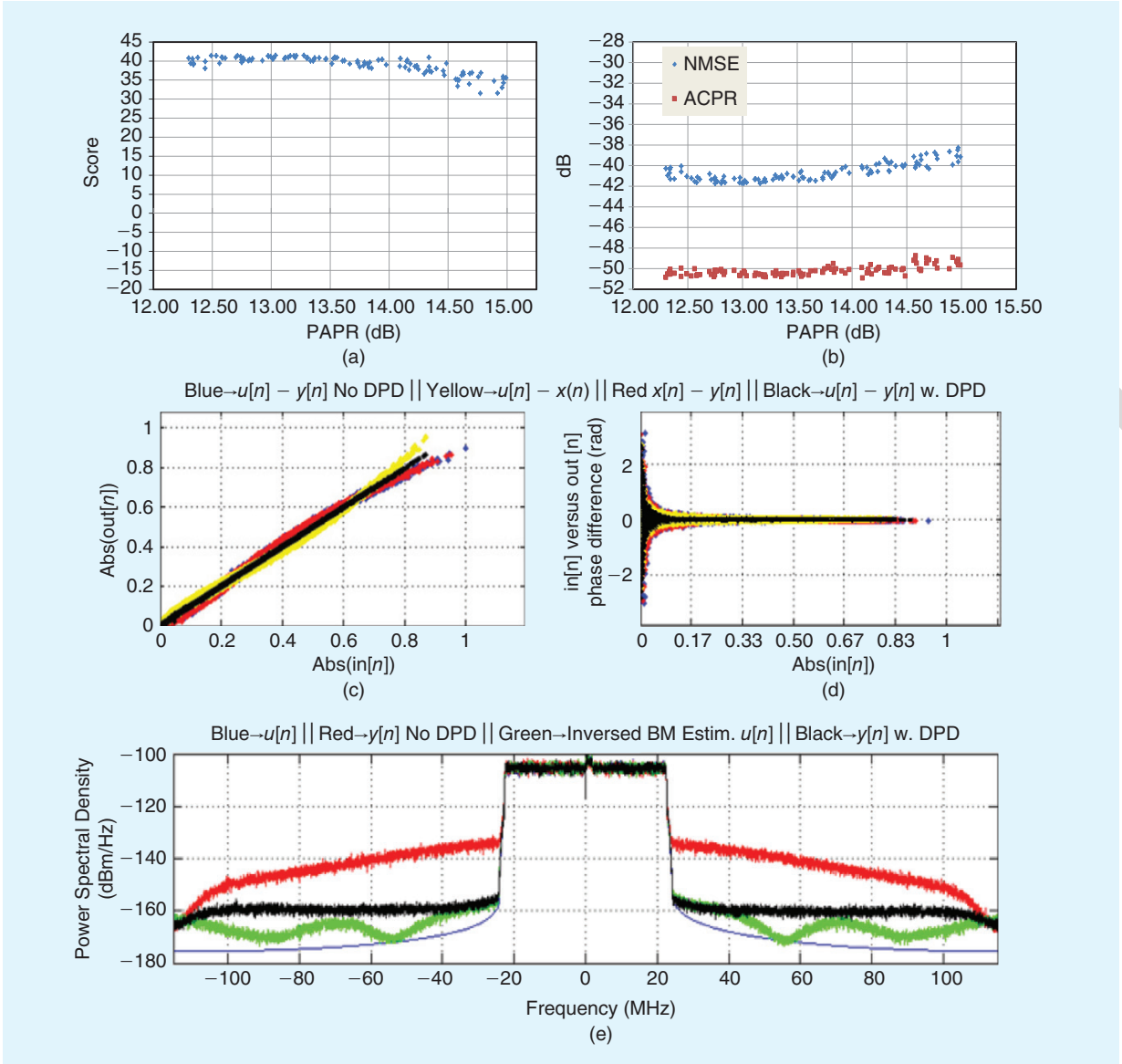

Figure 8. ***<Au: Please revise caption so that (a)-(e) are each clearly identified, as per magazine style.>*** *The AM-AM, AM-PM ,and spectra after DPD training (bottom) and score scatter plot NMSE and ACPR for 100 Weblab experiments after applying BM* ***<Au: Please spell out "BM.">*** *and CFR strategies (top).*

parameters tuning and long training possible given the available time with the user's own test signals.

After this period, the final competition test signal (not known in advance) was loaded into the workspace and 15 minutes were given to apply the DPD coefficients and build the predistorted signal, the performance of which was evaluated with the measurement setup. The overall architecture shown in Figure 7 performs well in targeting good performance at reasonable speed (considering the time predefined for each stage of the final competition) using a high-end computer.

In the final competition, however, the teams had to bring their script on a USB memory stick and load them into a laptop featuring lower end specifications. That forced the deactivation of the DPD block in charge of waveform long-term effects mitigation. Similarly, the waveform expansion and mesh-selecting technique were deactivated due to the previously established time and computing limitations (i.e., for each LS iteration at which the DPD coefficients were updated, at least three to five iterations had to be realized by the waveform expansion and mesh-selecting block at Figure 7).

Further Considerations and Conclusions

The score achieved in the final competition was 39.1 points, which falls very close to the target value of 40 points. This is a remarkable result because a challenging test waveform with near 14.5-dB PAPR was employed by the organizers and the measurement time and computational resource limitations required disabling some DPD blocks. For future occasions the use of the PCA technique may help in partially overcoming time and resource constraints [18]. The CFR mechanism provided protection against the final test waveform, since the NMSE degradation was almost negligible; but preventing the ACPR degradation was highly beneficial.

The PA linearization through digital predistortion student design competition is an excellent opportunity for the competing teams to work on linearization solutions enhancing the performance of radio infrastructures, considering the technology constraints and challenges and the many tradeoffs involved in real-life application scenarios. In this work, we have presented some techniques targeting performance improvement and robustness against the strong nonlinear behavior and memory effects of a GaN PA under high PAPR OFDM-like bursty waveforms such as those in 4G/5G scenarios. The proposed schemes increase the computational resources required in baseband processing and signal conversion stages, but nonetheless can be combined with resource minimization strategies like PCA or mesh-selecting.

Acknowledgments

The authors would like to gratefully thank Prof. Christian Fager, Prof. Thomas Eriksson, Dr. Koen Buisman, and Sebastian Gustafsson from Chalmers University of Technology; Dr. Per Landin from Ericsson; and Dr. Takao Inoue from National Instruments for their effort in preparing the competition and building the Weblab, a wonderful initiative fostering research in digital linearization and enabling worldwide access to state-of-the-art instrumentation.

This work has been partially supported by the Generalitat de Catalunya under grant 2014 SGR 1551; the Spanish Government and FEDER under MINECO projects TEC2014-58341-C4-3-R, TEC2014-58341-C4-4-R, and TEC2011-29126-C03-02; and the European Union under the project Network of Excellence in Wireless Communications (Newcom#), grant agreement 318306.

References

[1] B. Debaillie and C. Desset. (Aug. 2015). Power modeling of base stations. 5GrEEn Summerschool. Stockholm, Sweden. [Online]. Available: http://wireless.kth.se/5green/wp-content/uploads/sites/19/2014/08/BDebaille.pdf

[2] H. Gandhi, D. Greenstreet, and J. Quintal. (Aug. 2015) Digital radio front-end strategies provide game changing benefits for small cell base station. White Paper. [Online]. Available: http://www.ti.com/lit/wp/spry236/spry236.pdf

[3] (Aug. 2015). IMS 2015 student design competitions. *IEEE Microwave Theory Tech. Soc.* [Online]. Available: http://www.ims2015.org/students-main/student-design-competitions **<AU: Please provide the author name and volume number.>**

[4] C. Fager, T. Eriksson, K. Buisman, S. Gustafsson, and P. Landin. (Aug. 2015). Power amplifier linearization through digital predistortion (DPD). *IMS Student Des. Competition*. [Online]. Available: http://dpdcompetition.com/

[5] J. Kim and K. Konstantinou, "Digital predistortion of wideband signals based on power amplifier model with memory," *Electron. Lett.*, vol. 37, no. 23, pp. 1417–1418, Nov. 2001.

[6] A. Zhu, J. C. Pedro, and T. J. Brazil, "Dynamic deviation reduction based Volterra behavioral modeling of RF power amplifiers," *IEEE Trans. Microwave Theory Tech.*, vol. 54, no. 12, pp. 4323–4332, Dec. 2006.

[7] D. R. Morgan, Z. Ma, J. Kim, M. G. Zierdt, and J. Pastalan, "A generalized memory polynomial model for digital predistortion of RF power amplifiers," *IEEE Trans. Signal Processing*, vol. 54, no. 10, pp. 3852–3860, Oct. 2006.

[8] R. N. Braithwaite, "General principles and design overview of digital predistortion," *Chapter in Digital Processing for Front End in Wireless Communication and Broadcasting*, F. Luo, Ed. Cambridge, U.K.: Cambridge Univ. Press, 2011, pp. 143–191.

[9] R. N. Braithwaite, "A comparison of indirect learning and closed loop estimators used in digital predistortion of power amplifiers," in *Proc. IEEE MTT-S Int. Microwave Symp.*, May 17–22, 2015, pp. 1–4.

[10] H. Paaso and A. Mammela, "Comparison of direct learning and indirect learning predistortion architectures," in *Proc. IEEE Int. Symp. Wireless Communication Systems*, Reykjavik, Iceland, Oct. 2008, pp. 309–313.

[11] A. Zhu, P. J. Draxler, C. Hsia, T. J. Brazil, D. F. Kimball, and P. M. Asbeck, "Digital predistortion for envelope-tracking power amplifiers using decomposed piecewise Volterra series," *IEEE Trans. Microwave Theory Tech.*, vol. 56, no. 10, pp. 2237–2247, Oct. 2008.

[12] J. Wood, *Behavioural Modeling and Linearization of RF Power Amplifiers*, Norwood, MA: Artech House, 2005.

[13] A. S. Tehrani, T. Eriksson, and C. Fager, "Modeling of long term memory effects in RF power amplifiers with dynamic parameters," *IEEE MTT-S Int. Microwave Symp. Digest*, vol. 2, pp. 955–957, June 2012.
[14] P. L. Gilabert, G. Montoro, D. Lopez, N. Bartzoudis, E. Bertran, M. Payaro, and A. Hourtane, "Order reduction of wideband digital predistorters using principal component analysis," in *Proc. IEEE MTT-S Int. Microwave Symp. Dig.*, 2013, pp. 1–7.
[15] L. Guan and A. Zhu, "Optimized low-complexity implementation of least squares based model extraction for digital predistortion of RF power amplifiers," *IEEE Trans. Microwave Theory Tech.*, vol. 60, no. 3, pp. 594–603, 2012.
[16] T. Wang, P. L. Gilabert, and G. Montoro, "Under-sampling effects and computational cost reduction in RF power amplifier behavioral modeling," in *Proc. European Microwave Integrated Circuits Conf.*, Paris, France, Sept. 2015. **<AU: Please provide the page range.>**
[17] W.-J. Kim, K.-J. Cho, S. P. Stapleton, and J.-H. Kim, "An efficient crest factor reduction technique for wideband applications," *Analog Integr. Circ. Signal Proc.*, vol. 51, no. 1, pp. 19–26, Apr. 2007.
[18] D. Lopez, P. L. Gilabert, G. Montoro, and N. Bartzoudis, "Peak cancellation and digital predistortion of high-order QAM wideband signals for next generation wireless backhaul equipment," in *Proc. Int. Workshop Integrated Nonlinear Microwave Millimetre-wave Circuits*, Apr. 2014, pp. 1–3.

Callouts:

DPD relies on digitally cascading a nonlinear system before the PA, which provides an inverse response to the PA that then provokes a linear response at the output of the cascaded system, including the PA.

The student teams had to predistort 40-MHz BW signals at the output of a GaN PA operating at a 2.14-GHz carrier frequency and showing substantial memory effects due to trapping phenomena.

We built a statistical characterization block giving information about the waveform PAPR distribution that stores test signals for predefined PAPR ranges of interest.

The score achieved in the final competition was 39.1 points, which falls very close to the target value of 40 points.

The proposed schemes increase the computational resources required in baseband processing and signal conversion stages, but nonetheless can be combined with resource minimization strategies like PCA or mesh-selecting.